

# Part-based 3D Multi-person Tracking using Depth Cue in a Top View

Cyrille Migniot and Fakhreddine Ababsa

*IBISC Laboratory - University of Evry val d'Essonne, Evry, France*

**Keywords:** Gesture Tracking, Depth Cue, Particle Filter, Body Part, Multi-target Tracking.

**Abstract:** While the problem of tracking 3D human motion has been widely studied, the top view is never taken into consideration. However, for the video surveillance, the camera is most of the time placed above the persons. This is due to the human shape is more discriminative in the front view. We propose in this paper a markerless 3D human tracking on the top view. To do this we use the depth and color image sequences given by a kinect. First a 3D model is fitted to these cues in a particle filter framework. Then we introduce a process where the body parts are linked in a complete 3D model but weighted separately so as to reduce the computing time and optimize the resampling step. We find that this part-based tracking increases the accuracy. The process is real-time and works with multiple targets.

## 1 INTRODUCTION

One of the fundamental problems in computer vision is estimating the 3D motion of humans. A lot of research has been devoted to develop markerless methods which can track the motion of characters without interfering. The great majority of the methods in the literature use a model adapted to a front view of the person because the shape of a person is much more discriminative on this orientation. Furthermore the color of the skin and the elements of the face is seldom available in a top view. But the top view is often used in video-surveillance so as to better separate the persons, reduce the occlusions and evaluate the displacement of persons. The well known Viola-Jones face detector (Viola and Jones, 2004) provides for example an accurate estimation of faces localization in the front view. Nevertheless, in the application of the video-surveillance, the camera is frequently installed above the persons. The tracking on a top view needs a feature more descriptive than color: the depth. The kinect is one of the more popular devices used to provide it. It has sensors that capture both rgb and depth data. Here, we simulate the installation of kinect cameras in the ceiling of a supermarket. The goal is to analyze the behaviors of the customers during their buying acts within the shelves. The first step is tracking the pose of a customer. Then existing treatments could be adapted to our particular context for human activity recognition (Xu et al., 2012; Escalera, 2012).

Particle filtering (Isard and Blake, 1998a) provides a robust Bayesian framework for human mo-

tion capture. It estimates the current pose from a sample of possible states weighted from a likelihood function that represents the probability that a model corresponds to the observation (here the depth and the rgb image). As a person is articulated, most of tracking methods use as model a skeleton that comprises of a set of appropriately assembled geometric primitives (Deutscher and Reid, 2005; Hauberg et al., 2010; Horaud et al., 2009). Variations on the framework come from the choice of the likelihood function. Skin color (Gonzalez and Collet, 2011) and contour (matched to the chamfer distance (Xia et al., 2011)) are the most useful features. Kobayashi (Kobayashi et al., 2006) inserts results of classifiers in the likelihood function.

Some new methods introduce optimization at the propagation level. Shan (Shan and Wei, 2007) uses a Mean-Shift to place the particles in local minima of the likelihood function. Nevertheless, new particle set can not be used directly for particle filtering otherwise the whole concept of a Bayesian approach would be lost. But it can be used without destroying the original distribution by adopting the technique called importance sampling (Isard and Blake, 1998b). Importance sampling is too used by Cai (Cai et al., 2006) and by Bray (Bray et al., 2004) with a Stochastic Meta-Descent optimization. ISPF (Li et al., 1998) incrementally draws particles and uses an online learned pose estimator to iteratively tune them to their neighboring best states.

All poses of the skeleton are not possibles in practice. For example the head can not rotate over  $360^\circ$ .

The sampling can be constrained by a projection on the feasible configuration space (Hauberg et al., 2010) or by stochastic Nelder-Mead simplex search (Lin and Huang, 2004).

Finally, transformation can be applied to provide an unimodal likelihood model that allows using a Kalman filter. Larsen (Larsen et al., 2011) uses stereo data to disambiguate depth and Brox (Brox et al., 2010) tracks interest points provided by SIFT.

The likelihood function computing is the most time consuming operation because it has to be done once at every time step for every particle. Some adaptations are needed to obtain a real time processing. Gonzales (Gonzalez and Collet, 2011) realizes a tracking for each sub-part of the body so as to use only simple models. A hierarchical particle filter (Yang et al., 2005) simplifies the likelihood function. The annealed particle filtering (Deutscher and Reid, 2005) reduces the required number of particles. (Navarro et al., 2012) use layered particle filters to realize the tracking of pixels of skin from multiple views. Finally Kjellström (Kjellström et al., 2010) considers interaction with objects in the environment to constrain the pose of body and remove degrees of freedom.

In this paper, we describe a human gesture tracking from a top view by particle filtering. Relevant information is given by the depth provided by a kinect. The skeleton allows to model the interaction and the links into body parts. But the large number of degrees of freedom leads to a too large possible states representation to be well sampled by the particle filtering. Our main contributions are first to introduce adapted weighting of each degree of freedom depending on the part of the body that it is related to. Secondly, we use our treatment in the top view that is a seldom studied perspective but often used in the video surveillance or buying behavior context. Finally we transpose our method to the multi-target tracking.

## 2 PARTICLE FILTER IMPLEMENTATION

### 2.1 Observation

The Xtion Pro-live camera produced by Asus is used to simultaneously acquire the depth and the color cues. All the points that the sensor is not able to measure depth are offset to 0 in the output array. We regard it as a kind of noise. Moreover we only model the up part of the body. Thus, we threshold the image to only take into consideration the pixels recognized as an element of the torso, arms or head. It provides a

first segmentation of region of interest (ROI). A calibration step associates each pixel of the depth image to its corresponding in the color image.

One of the most interesting advantages of employing depth is the possibility of matching model and observation in the 3D space. A pixel  $p$  visible on the depth image can be expressed in two ways : in the 2D space of the image (figure 1(left)) and in the 3D space (figure 1(right)). In the 2D spatial space, the point is defined by:  $p^{2D} = \{x^{2D}, y^{2D}, d\}$  where  $x^{2D}$  and  $y^{2D}$  are the position of the pixel on the depth image and  $d$  is the depth value of this pixel. Calibration parameters computed by learning provide its corresponding in the 3D space defined by:  $p^{3D} = \{x^{3D}, y^{3D}, z^{3D}\}$ .

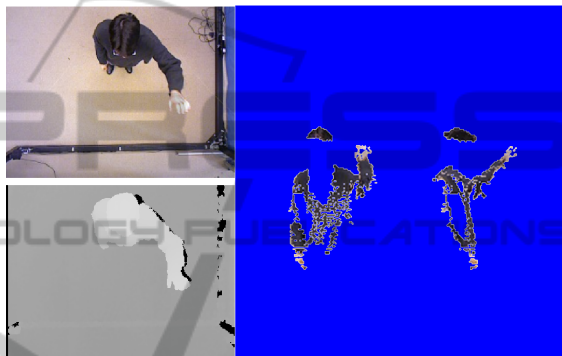


Figure 1: The kinect records simultaneously color and depth images (on the left). Each pixel visible in the 2D space of these images can be transposed in the spatial 3D space (on the right with projections on the XZ and YZ planes).

### 2.2 The Particle Filter

The particle filter, also called CONDENSATION (Isard and Blake, 1998a), is a method based on the Monte-Carlo simulation that provides a suitable framework for state estimation in a nonlinear, non-Gaussian system. At moment  $k$ , let  $x_k$  be the state of the model and  $y_k$  be the observation. Particle filter recursively approximates the posterior probability density  $p(x_k|y_k)$  of the current state  $x_k$  evaluating observation likelihood based on a weighted particle sample set  $\{x_k^i, \omega_k^i\}$ . Each of the  $N$  particles  $x_k^i$  corresponds to a random state propagated by the dynamic model of the system and weighted by  $\omega_k^i$ . There are 4 basic steps:

- **resampling:**  $N$  particles  $\{x_k^i, \frac{1}{N}\} \sim p(x_k|y_k)$  from sample  $\{x_k^i, \omega_k^i\}$  are resampled: large weight particles are duplicated while low weight particles are deleted.
- **propagation:** particles are propagated using the dynamic model of the system  $p(x_{k+1}|x_k)$  to obtain  $\{x_{k+1}^i, \frac{1}{N}\} \sim p(x_{k+1}|y_k)$ .

- **weighting:** particles are weighted by a likelihood function that defines the correspondence between the model and the new observation. The new weights  $\omega_{k+1}^i$  are normalized so that :  $\sum_{i=1}^N \omega_{k+1}^i = 1$ . It provides the new sample  $\{x_{k+1}^i, \omega_{k+1}^i\} \sim p(x_{k+1}|y_{k+1})$ .
- **estimation:** the new pose is approximated by:
 
$$x_{k+1} = \sum_{i=1}^N \omega_{k+1}^i x_{k+1}^i$$

### 2.3 The 3D Model

Our study focuses on the part of the body from the hip to the head that is visible in a top view. Our model is a skeleton with 6 rigid parts (figure 2(a)): the head, the torso with the shoulders, each arm and each forearm with the hand. We make the hypothesis that the neck has 2 degrees of freedom, each shoulder has 3 degrees of freedom and each elbow has 2 degrees of freedom (figure 2(c)). The pose of the torso is determined by 3 spatial coordinates and a rotation at the pelvis level (if the customer is bent down to catch a product at the bottom of the shelf). Overall, our 3D model has 17 degrees of freedom. That represents a very large possible states space that is hard to well-sample with a little number of particles and low time-processing. The state vector that defines the pose of the model is given by:  $V^{3D} = \{x^t, y^t, z^t, \theta^z, \theta_x^{ne}, \theta_z^{ne}, \theta_x^{r.sh}, \theta_y^{r.sh}, \theta_z^{r.sh}, \theta_x^{r.el}, \theta_z^{r.el}, \theta_x^{l.sh}, \theta_y^{l.sh}, \theta_z^{l.sh}, \theta_x^{l.el}, \theta_z^{l.el}\}$ . To represent the volume, geometrical primitives are added. Arms and forearms are modeled by truncated cylinders, torso by an elliptic cylinder and finally the hands by rectangular planes (figure 2(b)).

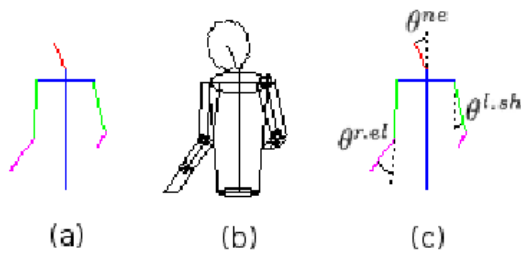


Figure 2: Our 3D model: skeleton is composed of 6 rigid parts (a), geometrical primitives form the volume (b) and angles related to the articulations define the pose (c).

#### 2.3.1 The Depth-based Likelihood

In the weighting process, the likelihood function gives the probability that a state of the model corresponds to the pose of the person. A particle defines a 3D model pose and the pixel of the depth image provides a set of

3D points  $\Delta^{3D}$ . The likelihood function describes the matching between these two 3D datasets. Let  $d_i^{ch}$  be the average 3D euclidean distance from the points of  $\Delta^{3D}$  to the model state defined by the particle  $i$ . The likelihood function is defined by :

$$\omega^i = e^{-d_i^{ch}} \quad (1)$$

#### 2.3.2 The Color-based Likelihood

While the color is not discriminative of human class, it gives interesting hint on the body parts. Indeed the color of each part (color of the hair, of the skin, of the clothes, etc.) is constant in the time. We define the color-based likelihood with the Bhattacharyya distance (Nummiaro et al., 2002). For each part, a color histogram is computed for each particle and compared with the one computed for the estimation at the previous instant. The sum of the corresponding Bhattacharyya distance is named  $d_i^{bh}$ . The likelihood function of equation 1 is updated by:

$$\omega^i = e^{-(d_i^{ch} + d_i^{bh})} \quad (2)$$

### 2.4 The Part-based Tracking

A part-based study has various advantages. First, the number of pixels visible on a top view for each part is not well-balanced: most of the pixels of ROI belong to the head or the shoulders. Thus, good positions of the head and the shoulders have most importance in the weighting and the resampling do not well follow the positions of the arms. Separating the weighting of each part provides a relevant estimation for each ones. Secondly, the number of degrees of freedom related to a part is lower than the one of the whole model. Hence, a lowest number of particles is required and the computing time is reduced.

We separate the model in 5 parts  $\mathcal{P}$ : the head, the top part of the shoulders, the torso and each arm (figure 3). Each of the 17 degrees of freedom is related to one part in table 1.

Table 1: Set of degrees of freedom related to each part.

Part	Degrees of freedom
Head	$\theta_x^{ne}, \theta_z^{ne}$
Shoulders	$x^t, y^t, z^t$
Torso	$\theta_x^{to}, \theta_z^{to}$
Right arm	$\theta_x^{r.sh}, \theta_y^{r.sh}, \theta_z^{r.sh}, \theta_x^{r.el}, \theta_z^{r.el}$
Left arm	$\theta_x^{l.sh}, \theta_y^{l.sh}, \theta_z^{l.sh}, \theta_x^{l.el}, \theta_z^{l.el}$

For a particle  $i$  and a part  $p$ , the weight  $\omega^{i,p}$  is defined by the depth and color-based likelihood function as previously but for the pixels of ROI whose  $p$  is the

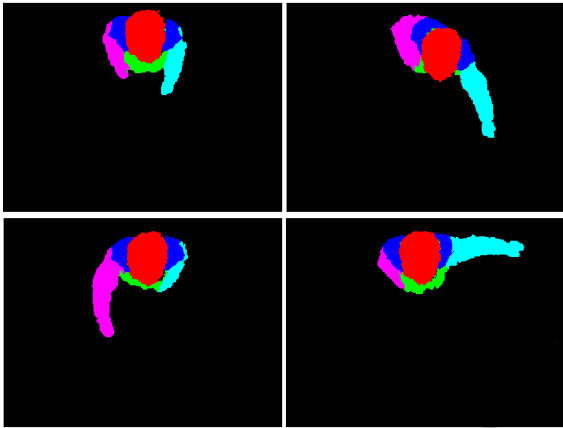


Figure 3: Each pixel of the ROI is associated with the nearest part of the model. The five parts are: the head (in red), the top part of the shoulders (in blue), the torso (in green), the right arm (in magenta) and the left arm (in cyan).

nearest part for the model state given by  $i$  in the 3D space. The sample is now defined by:

$$\{x_k^i = [x_k^{i,p}, p \in \mathcal{P}], \omega_k^i = [\omega_k^{i,p}, p \in \mathcal{P}]\} \quad (3)$$

In the resampling step, as we have different weights for each part, the elements  $x_k^{i,p}$  duplicated or deleted do not correspond to the same particles. Moreover, the combination of tested poses have to be diversified. That's why we shuffle each part of the state vector. The new sample is defined by:

$$\{x_k^i = [x_k^{f^p(i),p}, p \in \mathcal{P}], \omega_k^i = [\omega_k^{f^p(i),p}, p \in \mathcal{P}]\} \quad (4)$$

where  $f^p$  is a permutation from  $[1, N]$  to  $[1, N]$ .

### 3 PERFORMANCES

Two sequences with various motion of the arms are used to test the robustness and efficiency of our tracking algorithm. The first one ( $S_1$ ) is made of 450 frames ( $>1$ min) and follows the movements of a person with dark clothes. Indeed, most of the time, people wear dark clothes that are not easy to distinct from the other elements. But we want to estimate the influence of the color in the process. Therefore, the second sequence ( $S_2$ ) is made of 300 frames ( $\approx 43$ s) and follows the movements of a person with flashy clothes. These sequences are recorded in experimental conditions with a Xtion Pro live camera produced by Asus and installed 2.9 m from the floor that corresponds to the top of the shelves of a supermarket and is relevant with the depth sensor range (between 0.8m and 3.5m).

The fitting between the estimation and the observation is first visualized by the projection of the estimated model state on the color image (figure 4 on the

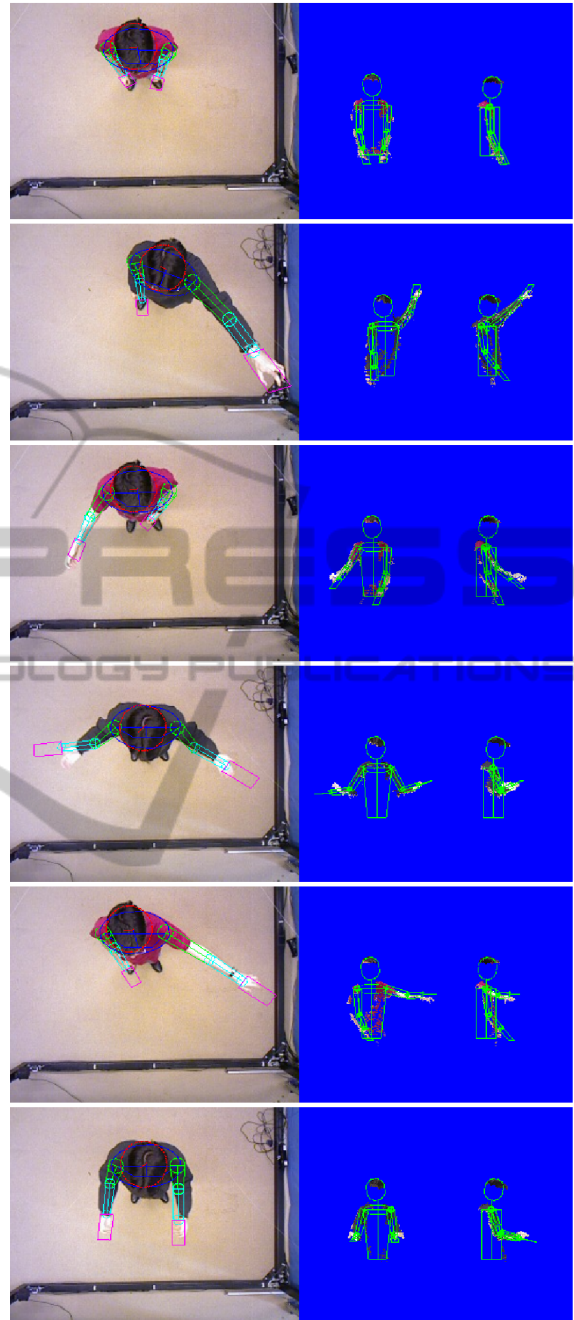


Figure 4: The tracking provides the pose of the person: on the left the model in the color image and on the right the model in the 3D space (the pixels in white correspond to the points given by the depth image).

left) and on the 3D space (figure 4 on the right). We note the good correspondence of our results and the efficient pose description by our 3D model.

To assess the accuracy of our method and estimate the improvement provided by the part-based processing, we need to quantitatively evaluate our results. We

want that the 3D points corresponding to the pixels of the person in the depth image are the closest of the 3D model state. However the arms are the most difficult part to track. The head and shoulders represents the most of the pixels and are rather well tracked. That leads to biases the evaluation. Thus we evaluate here only the tracking of the arms. The set of pixels of the arms  $\Delta_{arms}$  are manually annotated on all the frames of the two sequences to create a groundtruth. Then let  $\epsilon$  be the average 3D euclidean distance between the points of  $\Delta_{arms}$  and the estimated model state. A low value of  $\epsilon$  indicates a good correspondence between the model and the observation and a good estimation. A large number of particles best samples the possible states space and improves the estimation. Consequently increasing the number of particles improves the accuracy of the tracking. But it increases the computing time. We display the curve of  $\epsilon$  in a function of the average computing time for a frame so as to find an acceptable compromise. The processing times are obtained with a non-optimized C++ implementation running on a 3,1GHz processor.

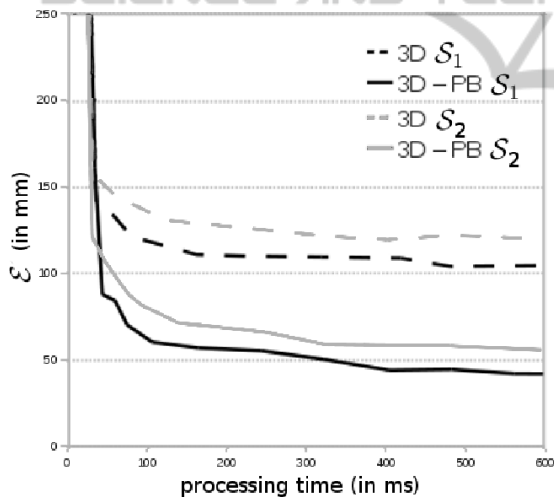


Figure 5: Performances of the two models on the sequences  $S_1$  et  $S_2$ . The part-based process improves the tracking.

The figure 5 shows explicitly that using a part-based process improves the tracking. The results are stable over the same computing time (approximately 150ms) but are much more accurate with the part-based process. Then, adding the color cue slightly improves the tracking (figures 6). It is more obvious on the 3D model. Indeed the color cue recognizes the various parts of the person that is already done by the part-based 3D model. The improvement produced by the color cue clearly depends on the video features: it is most marked when the colors are more flashy as in sequence  $S_2$ .

The particle survival rate  $\alpha$  denotes if the weights

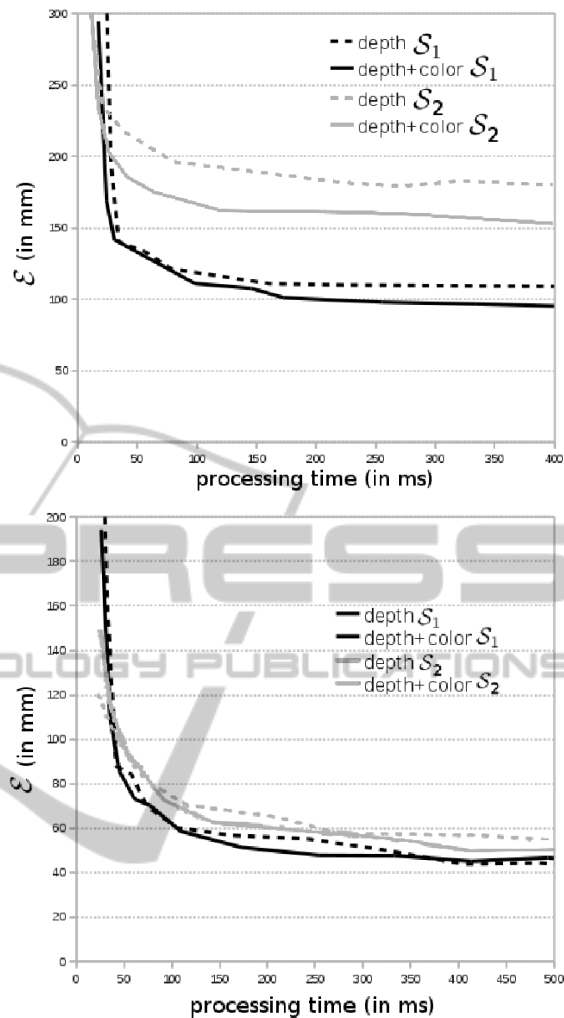


Figure 6: Performances with and without the color cue on the 3D (top) and the part-based 3D (bottom) models tracking. In favorable case (sequence  $S_2$ ), adding the color cue increases slightly the accuracy of the tracking and particularly with the 3D model.

of the particle are equally divided or not. A low value of  $\alpha$  means that a little number of particles are favored by the weighting. That increases the resampling process. In the figure 7, we notice that the arms are the fewer rate. Thus the likelihood function is the more efficient for these parts. Indeed it is for the arms that the 3D shape is the more descriptive. Moreover the color cue increases the description but decreases the efficiency of the likelihood function.

#### 4 MULTI-PERSON TRACKING

Multi-target tracking has been studied extensively in the literature to estimate the position of a person but

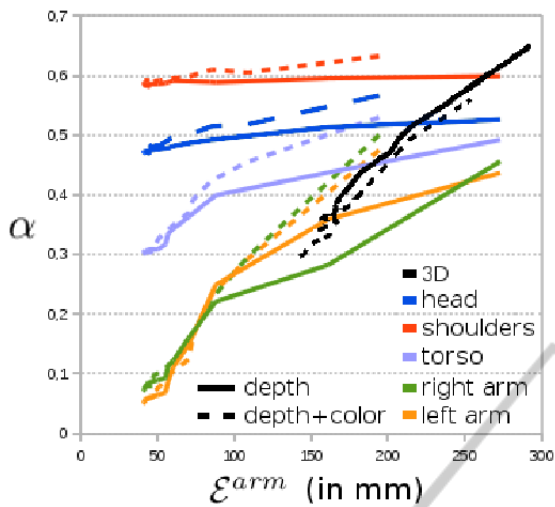


Figure 7: Particle survival rate evolution on the 3D model (in black) and for each part of the part-based 3D model: the arms are the most descriptive parts and adding the color cue decreases the efficiency of the likelihood function.

not to estimate his gesture. Object tracking that usually deals with targets of identical appearance, can be ranged by learning individual target models (Breitenstein et al., 2011; Shu et al., 2012; Liem and Gavril, 2009; Wu and Nevatia, 2007) but using classifiers is time-consuming. To avoid the problem produced by the overlapping of different targets, Gonzales (Gonzalez and Collet, 2011) uses the exclusion principle introduced by MacCormick and Blake (MacCormick and Blake, 1999). At each step, the observation (the pixels of the recorded image) is split between the targets. Xing (Xing et al., 2009) selects the best subset of current observations which corresponds to visible parts to update particle weights. Blocking methods penalize particles that overlap zones with other targets (Canton-Ferrer et al., 2008). Hence each tracker is associated to the relevant observation and can be performed almost independently.

Concatenating the data of the all targets in a single state vector increases dramatically the complexity of the system and the computing time. Applying the exclusion principle to track each target independently is relevant to obtain a real-time processing. For each moment  $k$  and target  $t$ , a prediction of the model state  $\hat{x}_{t,k}$  is computed from the previous estimation  $x_{t,k-1}$  and the dynamic of the system. Each prediction defines a 3D shape related to a model state. Let  $\mathcal{T}$  be the set of tracked targets. We assign each pixel of the observation (ROI) to the target whose the model state is the nearest in the 3D space. The assignation  $a(u)$  of the pixel  $u$  is defined by:

$$a(u) = \underset{t \in \mathcal{T}}{\operatorname{argmin}}(d_E(u, \hat{x}_{t,k})) \quad (5)$$

where  $d_E$  is the euclidean distance from a point to a model state in the 3D space.

With this configuration, the tracking of each person is processed as previously (figure 8).

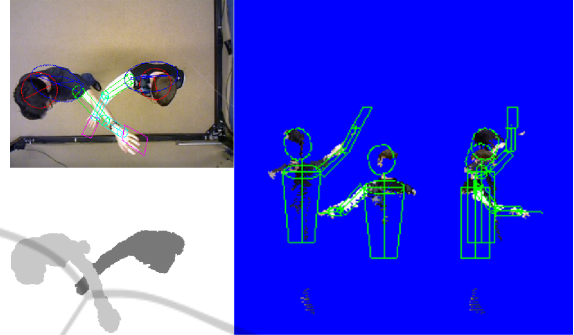


Figure 8: To deal with multi-person tracking, the observation corresponding to each target is split (bottom left). Then each target is tracked as previously.

We have recorded a new sequence  $S_3$  of 214 frames ( $\approx 30s$ ) that contains two persons whose the arms are frequently crossing and overlapped. That causes inter-person occlusions. On this sequence, the rate of correctly assigned pixel of the ROI  $\Delta^{3D}$  is 99,56%.

In practice, the tracking will be used for behavior recognition. The main challenge is to define the acts of the person. In the multi-target tracking, it means that the spatial proximity between two targets and the possible inter-person occlusion it causes must not per-

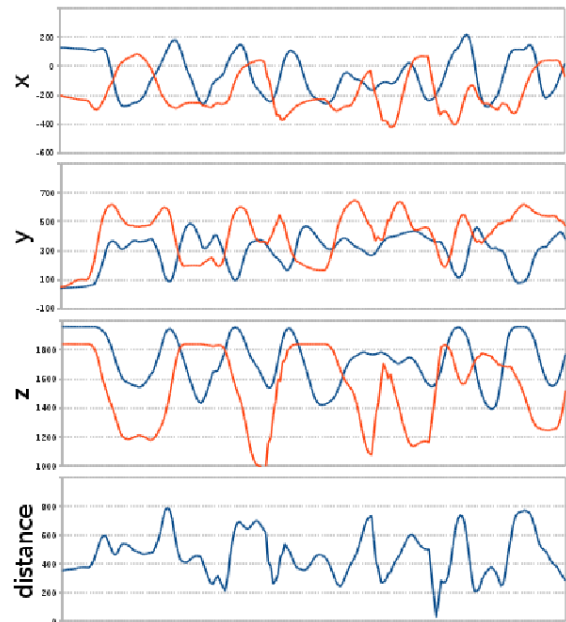


Figure 9: Evolution on our estimation of the location of the moving wrist for the two persons in the  $x$ ,  $y$ ,  $z$  coordinates and of the distance between the two wrists. Thanks to the exclusion principle, the two targets are tracked independently.

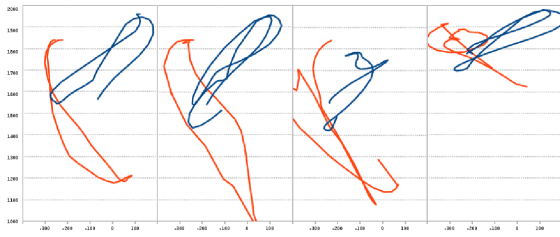


Figure 10: Trajectories of the moving wrist for the two persons on our estimation projected in the XZ plane during the four quarters of the sequence  $S_3$ . The two arms often overlap in the recorded 2D image but they are correctly tracked in the 3D space.

turbs the movement estimation of each target. Consequently, we have displayed the evolution over time of the 3D location of the wrists (well-descriptive of the arm movement) of the two persons in sequence  $S_3$  (figures 9 and 10). We notice that the method keep tracking the arm regularly in case of occlusion and that the two trajectories have independant evolutions.

## 5 CONCLUSIONS

In this paper we have proposed a new 3D tracking method based on the well known particle filter method. To be efficient in the particular case of the top view, the new Asus camera records the depth and color cue. Then we have introduced a particle filtering where the elements of the state vector are weighted separately but linked by the complete 3D model. Experimental results show that this part-based process improves the efficiency of the tracking. The resulting application is real time and works for multi-person tracking by the application of the exclusion principle.

The color of the skin visible for the hands is well descriptive of the human class. The detection of the hands could constraint the model in future works and reduce the number of degrees of freedom. Then, the tracking is only the first step of the human behavior. Our method could be introduced in an action recognition process. A camera pose estimation (Didier et al., 2008; Ababsa and Mallem, 2008; Ababsa, 2009) could insert our work in a Augmented Reality context with a moving camera. Finally a coupled tracking and segmentation method would give more information for the following of the processing and prevent wrong estimations of each of the two treatments.

## REFERENCES

- Ababsa, F. (2009). Robust extended kalman filtering for camera pose tracking using 2d to 3d lines correspondences. *IEEE/ASME Conference on Advanced Intelligent Mechatronics*, pages 1834–1838.
- Ababsa, F. and Mallem, M. (2008). A robust circular fiducial detection technique and real-time 3d camera tracking. *International Journal of Multimedia*, 3(4):34–41.
- Bray, M., Koller-Meier, E., and Van Gool, L. (2004). Smart particle filtering for 3d hand tracking. *IEEE International Conference on Automatic Face and Gesture Recognition*, pages 675–680.
- Breitenstein, M., Reichlin, F., Leibe, B., Koller-Meier, E., and Van Gool, L. (2011). Online multiperson tracking-by-detection from a single, uncalibrated camera. *IEEE Transaction on Pattern Analysis and Machine Intelligence*, XXXIII:1820–1833.
- Brox, T., Rosenhahn, B., Gall, J., and Cremers, D. (2010). Combined region and motion-based 3d tracking of rigid and articulated objects. *IEEE Transaction on Pattern Analysis and Machine Intelligence*, pages 402–415.
- Cai, Y., De Freitas, N., and Little, J. (2006). Robust visual tracking for multiple targets. *European Conference on Computer Vision*, pages 107–118.
- Canton-Ferrer, C., Salvador, J., Casas, J. R., and Pardàs, M. (2008). Multi-person tracking strategies based on voxel analysis. *Multimodal Technologies for Perception of Humans*, pages 91–103.
- Deutscher, J. and Reid, I. (2005). Articulated body motion capture by stochastic search. *International Journal of Computer Vision*, 2:185–205.
- Didier, J., Ababsa, F., and Mallem, M. (2008.). Hybrid camera pose estimation combining square fiducials localisation technique and orthogonal iteration algorithm. *International Journal of Image and Graphics*, 8(1):169–188.
- Escalera, S. (2012). Human behavior analysis from depth maps. In *International Conference on Articulated Motion and Deformable Objects*, pages 282–292.
- Gonzalez, M. and Collet, C. (2011). Robust body parts tracking using particle filter and dynamic template. In *IEEE International Conference on Image Processing*, pages 529 – 532.
- Hauberg, S., Sommer, S., and Pedersen, K. S. (2010). Gaussian-like spatial priors for articulated tracking. In *European Conference on Computer Vision*, pages 425 – 437.
- Horand, R., Niskanen, M., Dewaele, G., and Boyer, E. (2009). Human motion tracking by registering anarticulated surface to 3d points and normals. *IEEE Transaction on Pattern Analysis and Machine Intelligence*, XXXI:158–163.
- Isard, M. and Blake, A. (1998a). Condensation - conditional density propagation for visual tracking. *International Journal of Computer Vision*, XXIX:5 – 28.
- Isard, M. and Blake, A. (1998b). Icondensation - unifying

- low-level tracking in a stochastic framework. *European Conference on Computer Vision*, I:893–908.
- Kjellström, H., Kragic, D., and Black, M. J. (2010). Tracking people interacting with objects. In *IEEE Conference on Computer Vision and Pattern Recognition*.
- Kobayashi, Y., Sugimura, D., Sato, Y., Hirasawa, K., Suzuki, N., Kage, H., and Sugimoto, A. (2006). 3d head tracking using the particle filter with cascaded classifiers. In *British Machine Vision Conference*, pages 37 – 46.
- Larsen, A., Hauberg, S., and Pedersen, K. (2011). Unscented kalman filtering for articulated human tracking. *Scandinavian conference on Image analysis*, pages 228–237.
- Li, M., Tan, T., Chen, W., and K., H. (1998). Efficient object tracking by incremental self-tuning particle filtering on the affine group. *IEEE Transactions on Image Processing*, XXI:1298–1313.
- Liem, M. and Gavrilu, D. (2009). Multi-person tracking with overlapping cameras in complex, dynamic environments. *British Machine Vision Conference*, pages 1–10.
- Lin, J.Y. Wu, Y. and Huang, T. (2004). 3d model-based hand tracking using stochastic direct search method. *IEEE International Conference on Automatic Face and Gesture Recognition*, pages 693–698.
- MacCormick, J. and Blake, A. (1999). A probabilistic exclusion principle for tracking multiple objects. *International Journal on Computer Vision*, I:572–578.
- Navarro, S., López-Méndez, A., Alcoverro, M., and Casas, J. R. (2012). Multi-view body tracking with a detector-driven hierarchical particle filter. In *International Conference on Articulated Motion and Deformable Objects*, pages 82–91.
- Nummiaro, K., Koller-Meier, E., and Van Gool, L. (2002). An adaptive color-based particle filter. *Image and Vision Computing*, XXI:99–110.
- Shan, C., T. T. and Wei, Y. (2007). Real-time hand tracking using a mean shift embedded particle filter. *Pattern Recognition*, XXXX:1858–1970.
- Shu, G., Dehghan, A., Oreifej, O., Hand, E., and Shah, M. (2012). Part-based multiple-person tracking with partial occlusion handling. *IEEE Conference on Computer Vision and Pattern Recognition*, pages 1815–1821.
- Viola, P. and Jones, M. (2004). Robust real-time face detection. *International Journal of Computer Vision*, LVII(2):137–154.
- Wu, B. and Nevatia, R. (2007). Detection and tracking of multiple, partially occluded humans by bayesian combination of edgelet based part detectors. *International Journal on Computer Vision*, LXXV:247–266.
- Xia, L., Chen, C.-C., and Aggarwal, J. K. (2011). Human detection using depth information by kinect. *International Workshop on Human Activity Understanding from 3D Data*.
- Xing, J., Ai, H., and Lao, S. (2009). Multi-object tracking through occlusions by local tracklets filtering and global tracklets association with detection responses. *IEEE Conf. on Computer Vision and Pattern Recognition*, pages 1200–1207.
- Xu, R., Agarwal, P., Kumar, S., Krovi, V. N., and Corso, J. J. (2012). Combining skeletal pose with local motion for human activity recognition. In *International Conference on Articulated Motion and Deformable Objects*, pages 114–123.
- Yang, C., Duraiswami, R., and Davis, L. (2005). Fast multiple object tracking via a hierarchical particle filter. In *International Conference on Computer Vision*, pages 212 – 219.